

Assessment of Lower Hybrid Current Drive System for COMPASS*

V. Fuchs, R. W. Harvey^{a)}, R. A. Cairns^{b)}, J. Urban, F. Žáček

Association EURATOM/IPP.CR, IPP AS CR, Za Slovankou 3, 18200 Prague 8

Y. Peysson, J. Decker, M. Preynas, M. Goniche, J. Hillairet

CEA, IRFM, Cadarache, 13108 St Paul lez Durance, France

Abstract

The Prague IPP recently acquired from UKAEA Culham the COMPASS tokamak together with an incomplete 1.3 GHz lower hybrid (LH) system [1]. A proposal for an alternative 3.7 GHz COMPASS LH multi-junction antenna was previously presented in Refs. [2, 3]. We present herein simulations of Lower Hybrid Current Drive (LHCD), in support of a choice between the 1.3 GHz and the 3.7 GHz LH systems. The LHCD simulations are carried out with state-of-the-art ray tracing/Fokker-Planck codes C3PO/LUKE [4, 5] and GENRAY/CQL3D [6, 7]. These two suites of codes are very different in terms of organization and applied numerical methods. Despite these differences, and despite the very wide principal spectral component of COMPASS antenna ($\Delta N_{\parallel}=1.7$ at 1.3 GHz, $\Delta N_{\parallel}=0.6$ at 3.7 GHz)—essentially at the limit of geometrical optics—the two codes give compatible results in terms of power deposition and LHCD efficiency.

1 Introduction

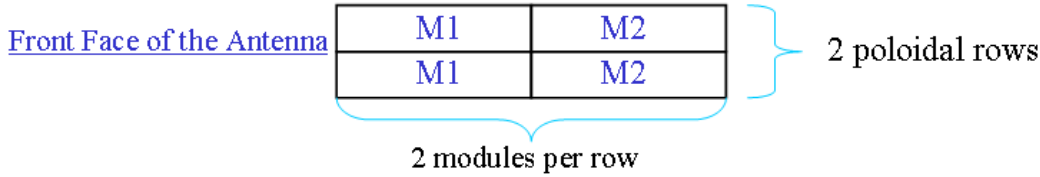
COMPASS is a compact size tokamak [1] with major radius $R_p = 0.576$ m, minor radius $r_a = 0.21$ m, operating at a toroidal magnetic field between 1.2 Tesla and 2.1 Tesla, and a plasma current between 0.1 MA and 0.25 MA. Two distinct operating MHD equilibria are foreseen, the first, termed SND, has low triangularity, $\delta \approx 0.4$. The second, termed SNT, has higher triangularity, $\delta \approx 0.7$. For the purpose of the present study, we consider 4 operation scenarios specified in **Table 1** below

Table 1 COMPASS operation scenarios foreseen for lower hybrid auxiliary heating and current drive (δ ... triangularity, κ ... elongation)

| Scenario | B_T [T] | I_p [kA] | δ | κ | n_{e0} [10^{19} m^{-3}] | T_{e0} [keV] |
|----------|------------|------------|------------|------------|---------------------------------------|----------------|
| SND-01 | 1.2 | 175 | 0.4 | 1.4 | 3.0 | 1.2 |
| SND-02 | 1.2 | 175 | 0.4 | 1.4 | 3.5 | 1.5 |
| SNT-01 | 2.1 | 250 | 0.7 | 1.5 | 3.0 | 1.1 |
| SNT-02 | 2.1 | 250 | 0.7 | 1.5 | 3.5 | 1.5 |

The IPP Prague installation of the COMPASS tokamak came from UKAEA CULHAM with a system capable of coupling about 200 kW of LH power to the plasma. The associated at 1.3 GHz slow wave launcher is a Brambilla-type 8-waveguide antenna (grill), but lacking power supplies and other

necessary hardware. A substantial investment is therefore necessary to render the system operational. As an alternative, CEA, IRFM has offered IPP Prague 2-3 of their older 3.7 GHz, 500 kW pulsed TED TH2103 klystrons to power a prospective new multi-junction antenna [2, 3] for COMPASS, shown schematically below:



Two klystrons would power the 2 sets of poloidally connected modules. Such a new LH system for COMPASS would likewise require a substantial investment into antenna construction and auxiliary hardware. Principal LH antenna properties which are of interest to lower hybrid current drive (LHCD) are their reflectivity (R) and directivity (D). For a typical COMPASS edge density of about 10^{18} m^{-3} the ALOHA antenna - plasma coupling code gives $R \approx 15\%$, $D \approx 70\%$ for the 1.3 GHz antenna, while for the 3.7 GHz antenna R is negligible and $D \approx 68\%$ [2, 3]. Section 2 gives results of ray-tracing/Fokker-Planck LHCD simulations for COMPASS at 1.3 GHz and 3.7 GHz from two different codes: section 2.1 gives results from the CP3O / LUKE code [4, 5], and section 2.2 gives LHCD results from the GENRAY / CQL3D [6, 7] code. Finally, section 3 gives our conclusions.

2 Ray-tracing / Fokker-Planck simulations

2.1 C3PO / LUKE results

A feature which distinguishes the C3PO/LUKE simulation method from all other similar LHCD codes is that C3PO traces just one ray (the central $N_{\parallel 0}$) per spectrum lobe and poloidal antenna row. Tables 2a, b and Fig. 1 show the principal results for plasma conditions of Table 1.

Table 2a Selected results for 90° waveguide phasing of the 1.3 GHz antenna, at 210 kW of LH input power. P_{LH} is the absorbed power and $\langle \rho_{\text{abs}} \rangle$ is the mean location of absorption.

| equilibrium | f [MHz] | $N_{\parallel 0}$ | P_{LH} [kW] | I_{LH} [kA] | η [A/w] | $\langle \rho_{\text{abs}} \rangle$ |
|---------------|------------|-------------------|----------------------|----------------------|--------------|-------------------------------------|
| SND-01 | 1.3 | 3.45 | 210 | 50 | 0.24 | 0.65 |
| SND-02 | 1.3 | 3.45 | 210 | 240 | 1.14 | 0.70 |
| SNT-01 | 1.3 | 3.45 | 210 | 50 | 0.24 | 0.65 |
| SNT-02 | 1.3 | 3.45 | 210 | 220 | 1.05 | 0.85 |

Table 2b Selected results for 90° waveguide phasing and 0° module phasing of the multi-junction 3.7 GHz antenna, at 500 kW of LH input power.

| equilibrium | f [MHz] | $N_{\parallel 0}$ | P_{LH} [kW] | I_{LH} [kA] | η [A/w] | $\langle \rho_{\text{abs}} \rangle$ |
|---------------|------------|-------------------|----------------------|----------------------|--------------|-------------------------------------|
| SND-01 | 3.7 | 2.5 | 500 | 150 | 0.30 | 0.20 |
| SND-02 | 3.7 | 2.5 | 500 | 450 | 0.90 | 0.45 |
| SNT-01 | 3.7 | 2.5 | 500 | 70 | 0.14 | 0.45 |
| SNT-02 | 3.7 | 2.5 | 500 | 260 | 0.52 | 0.60 |

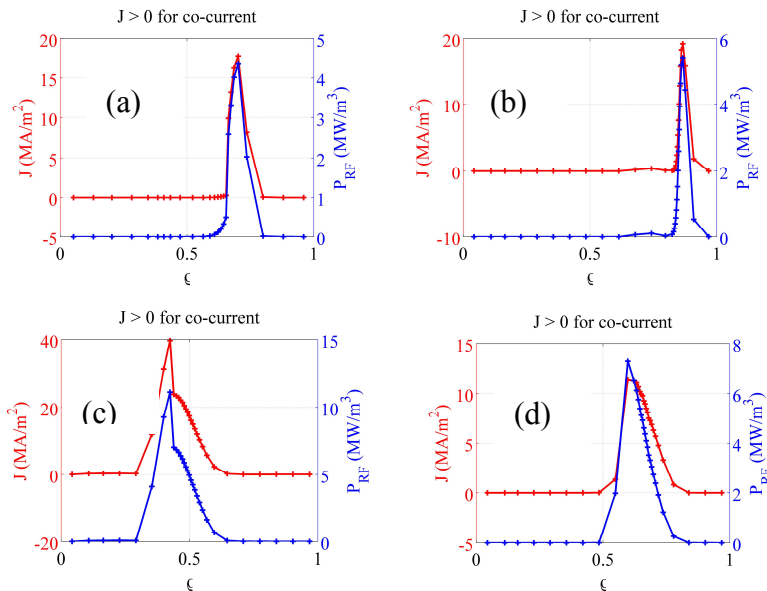


Fig. 1 Power deposition and current density profiles for $B_T=2.1\text{T}$ scenarios of Table 1
a) SND-02-f1p3, b) SNT-02-f1p3, c) SND-02-f3p7, d) SNT-02-f3p7

2.2 GENRAY / CQL3D results

Selected results are shown in Tables 3a, b, and in Fig. 2.

Table 3a Selected results for 90° waveguide phasing of the 1.3 GHz antenna, at 210 kW of LH input power.

| equilibrium | f [MHz] | $N_{\parallel 0}$ | P_{LH} [kW] | I_{LH} [kA] | η [A/w] | $\langle \rho_{\text{abs}} \rangle$ |
|---------------|------------|-------------------|----------------------|----------------------|--------------|-------------------------------------|
| SND-01 | 1.3 | 3.45 | 153 | 28 | 0.18 | 0.20, 0.70 |
| SND-02 | 1.3 | 3.45 | 196 | 170 | 0.87 | 0.25, 0.70 |
| SNT-01 | 1.3 | 3.45 | 206 | 127 | 0.61 | 0.35, 0.70 |
| SNT-02 | 1.3 | 3.45 | 209 | 201 | 0.96 | 0.35, 0.70 |

Table 3b Selected results for 90° waveguide phasing, 0° module phasing of the multi-junction 3.7 GHz antenna, at 500 kW of LH input power.

| equilibrium | f [MHz] | $N_{\parallel 0}$ | P_{LH} [kW] | I_{LH} [kA] | η [A/w] | $\langle \rho_{\text{abs}} \rangle$ |
|---------------|------------|-------------------|----------------------|----------------------|--------------|-------------------------------------|
| SND-01 | 3.7 | 2.5 | 447 | 388 | 0.84 | 0.20, 0.45 |
| SND-02 | 3.7 | 2.5 | 480 | 402 | 0.84 | 0.25, 0.60 |
| SNT-01 | 3.7 | 2.5 | 488 | 131 | 0.23 | 0.55 |
| SNT-02 | 3.7 | 2.5 | 495 | 360 | 0.73 | 0.20, 0.45 |

We note that the preferred operation condition for LHCD at both frequencies is at higher B_T -field (because of better LH wave accessibility). We also note that both codes give compatible current density profiles (except for the SND-02 case).

4 Conclusions

The 3.7 GHz multi-junction proves a better choice than the 1.3 GHz standard grill mainly because of its much smaller reflectivity in the $n > 2.5 \times 10^{17} \text{ m}^{-3}$ edge density range. An obvious advantage of the projected 3.7 GHz system is a much larger available operating power: 0.5 MW per klystron. Thus the 3.7 GHz system can easily supply the maximum allowable 0.5 MW (corresponding to the empirical antenna power density limit of 25 MW/m^2 [8]) to the plasma. The 3.7 GHz system also offers the

possibility of better comparison with other existing LH experiments in Europe (Tore Supra, JET). The estimated LHCD efficiencies are of the order of 0.5 – 1 A/W, depending on operation conditions. As a next step in the simulations, we plan to obtain self-consistent results for the LH power absorption and electron temperature profiles.

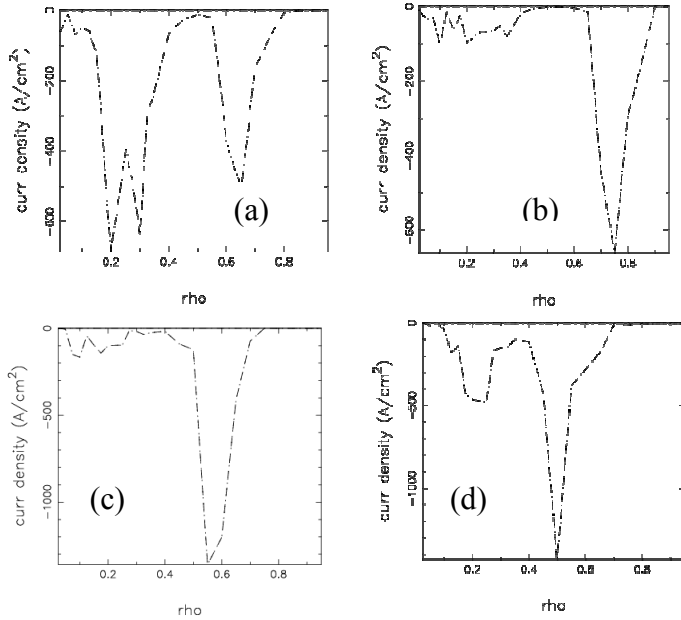


Fig. 2 Power deposition and current density profiles for $B_T=2.1\text{T}$ scenarios of Table 1
 a) SND-02-f1p3, b) SNT-02-f1p3, c) SND-02-f3p7, d) SNT-02-f3p7

Acknowledgments

We thank V. Pericoli-Ridolfini for valuable discussions.

References

- *Supported in part by Czech Republic Science Foundation Grant GA ČR 202/07/0044, AS CR AV0Z20430508, MSMT 7G09042, and USDOE ER54744.
- a) Permanent address: CompX, Del Mar, California 92014-5672, USA
- b) Permanent address: University of St Andrews, St Andrews, Scotland, UK
- [1] R. Pánek, O. Bilyková, V. Fuchs, et al., *Czech. J. Phys.* **56**, B125-B137, 2006
- [2] Mélanie Peysson, *Développement d'un nouveau module pour le code de couplage ALOHA*, Mémoire de Master, 31/07/2009, CEA Cadarache.
- [3] J. Hillairet, D. Voyer, A. Ekedahl, et al., *Nucl. Fusion* **50**, 125010, 2010
- [4] Y. Peysson and J. Decker, in X. Garbet, O. Sauter, and E. Sindoni, editors, *Theory of Fusion Plasmas*, Vol. **1069** of AIP Conference Proceedings, 2008, pp. 176–187.
- [5] Y. Peysson, J. Decker, and V. Basiuk, 34th EPS Conference on Plasma Physics, Warsaw, 2-6 July 2007, **Vol. 31F**.
- [6] R.W. Harvey, M.R. O'Brien, V.Rozhdestvesky, et al., *Phys. Fluids* **B5**, 446 (1993).
- [7] R.W. Harvey and M.G. McCoy, *The CQL3D Code*, Proc. IAEA TCM on Advances in Sim. and Modeling of Thermonuclear Plasmas, Montreal, (1992) p. 527; <http://www.compxco.com>.
- [8] Y. Peysson and the Tore Supra Team, *Nucl. Fusion* **41**, 1703, 2001